

# Vortex dynamics and skyrmions in four to six dimensions: Coherence vortices in Bose-Einstein condensates

Emil Lundh<sup>1</sup>

<sup>1</sup>*Department of Physics, Umeå University, 901 87 Umeå, Sweden*

(Dated: October 16, 2018)

I point out how coherence vortices, i.e., topological defects in a correlation function, could help explore new physics if they are created in matter waves. Vortex dynamics could be studied in up to six dimensions, and spin topological defects unseen in lower dimensions could be created. A rudimentary proof-of-principle experiment is sketched and simulated, in which three Bose-Einstein condensates are used to create and detect coherence vortices.

Coherence vortices is a concept first coined in optics research [1, 2]. These are phase singularities that exist not directly in a physical field, but in a spatial correlation function of a field. Typically, one may have a partially coherent field, such as a laser beam with limited coherence time, where the observed expectation value does not exhibit a phase singularity, but a double-slit interference experiment may reveal a phase winding around a singularity in the field-field correlation function. As such, coherence vortices are defined in a coordinate space with twice the dimensionality of the physical space. Simula and Paganin pointed out that this means that coherence vortices are possible in a one-dimensional system [3]; furthermore, they alluded to the possibility of observing coherence vortices in matter as well as in optics.

A vortex in a two-point correlation function suggests the intriguing prospect of studying vortex dynamics in up to six dimensions. However, for the study of *dynamics*, optical systems are impractical and one needs to turn to coherent matter waves – partially or fully Bose-Einstein condensed gases of ultracold atoms. Matter waves have several advantages as well as disadvantages with respect to optics when it comes to studying coherence vortices. Detection is a very different affair in matter waves, but it can be done, as will be discussed in detail below. Among the advantages are not only the possibility to study dynamics, but also the prospect of using multi-component condensates for creating higher-dimensional topological objects. A four- or six-dimensional space will offer new possibilities for these.

The purpose of this paper is to point out the new prospects for research that are made possible by coherence vortices in matter systems; notably, high-dimensional vortex dynamics and high-dimensional topological defects. In addition, I sketch and simulate a clumsy but doable scheme for the realization and detection of coherence vortices in a system of trapped cold bosons. I see this as a proof of principle, which helps open up the way towards six-dimensional vortex dynamics.

Let us first note that there exist already theoretical proposals that would in effect contain coherence vortices; namely the quantum fluctuating vortices studied by Mar-

tikainen and Stoof [4], and the slowly-rotating small Bose and Fermi systems studied by Reimann, Kavoulakis *et al.* [5, 6]. What these systems have in common is that the exact ground state would contain a vortex whose position is subject to quantum uncertainty. The symmetry will be broken and a definite vortex position is chosen by any finite symmetry-breaking potential; this destroys the superposition and thus the coherence vortex is reduced to an ordinary vortex. The scheme I describe below is more robust, though perhaps less elegant.

*System.* – Cold bosonic atoms are described by commuting field operators  $\psi_a(\mathbf{r})$ ,  $\psi_a^\dagger(\mathbf{r})$ , where  $a$  designates species and/or spin state  $(F, m_F)$ , and  $\mathbf{r}$  is the spatial coordinate vector. If the atoms form a Bose-Einstein condensate (BEC), the expectation of a single field is non-vanishing,  $\Psi_a(\mathbf{r}) = \langle \psi_a(\mathbf{r}) \rangle$ , and its expectation value is called the condensate wave function. The vortices supported by such wavefunctions are, of course, well studied [7]. Instead, we are here interested in phase singularities in the field-field correlation function,

$$g_{aa}(\mathbf{r}, \mathbf{r}') = \langle \psi_a^\dagger(\mathbf{r}) \psi_a(\mathbf{r}') \rangle, \quad (1)$$

which is a function of  $2 \times D$  coordinates, where  $D$  is the number of dimensions in which the atoms can move. Such phase singularities may exist also when there are none in  $\Psi_a(\mathbf{r})$ . Henceforth, we will be dropping the subscript  $a$  when we are dealing with only one component.

*Topological defects.* – In a single-component fluid in  $D$  dimensions, the only type of topological defect that can exist is a vortex, characterized by an integer phase winding number around a closed loop. Such a loop surrounds a phase singularity of dimension  $D-2$ , i.e., a point vortex in two dimensions or a vortex line in three dimensions. In  $D = 4$  the singularity lies on a two-dimensional (2D) surface, and it is helpful to imagine the full 4D space as a succession of 3D spaces, each (except in degenerate cases) containing a vortex line, whose trajectory varies continuously as we move between adjacent 3D spaces. A closed loop is drawn around the vortex line in one of the 3D spaces. If the loop is displaced by a sufficiently small amount in any direction, including the fourth, it will still encircle the singularity. Thus the 2D sheet retains the topological stability we associate with a vortex.

In a multi-component quantum fluid, higher-dimensional topological defects are possible, as is well known in the 3D case. The allowed topological defects in a given quantum fluid are classified using homotopy theory [8–10]: Let  $G$  be the symmetry group of the order parameter, and let  $H$  be the group of operations that leave a specific ground state invariant. Then the order parameter space  $M = G/H$  is in one-to-one correspondence with the set of distinct degenerate ground states of the system. Now the first homotopy group of  $M$ ,  $\pi_1(M)$ , gives the allowed topological defects that may be encircled by a ring; these are (singular) point defects in 2D, line defects in 3D, and planes in 4D. Likewise, the second homotopy group  $\pi_2(M)$  enumerates those topological defects that can be encircled by a spherical shell, and in 3D those are point defects, i.e., monopoles. For instance, in a single-component BEC,  $M = S^1$ , the circle; and we have  $\pi_1(S^1) = Z$ , where  $Z$  is the set of integers. These integers are the possible winding numbers for a vortex. It is now plain to see that in higher dimensions, there may be topological defects classified by higher-order homotopy groups, which do not make sense in lower dimensions – e.g.,  $\pi_3$  characterizes singular point defects in 4D or sheet defects in 6D. In a single-component BEC, again, all homotopy groups higher than 1 are zero;  $\pi_2(S^1) = \pi_3(S^1) = 0$  etc; which implies that the only topologically stable defect for such a fluid is the vortex. For the ferromagnetic state of a spin-1 condensate,  $M = \text{SO}(3)$ , and its homotopy groups are  $\pi_3(M) = Z$  and  $\pi_4(M) = \pi_5(M) = Z_2$ , where  $Z_2$  is the set of integers modulo 2. Further investigation of the homotopy groups associated with the correlation function matrices  $g_{ab}$  of the ground states in spinor condensates must be left to future studies.

*Creation.* – We now turn to the experimental creation and detection of coherence vortices. A number of ingredients are necessary for the creation, and a few more for the detection, of coherence vortices. First, one needs a non-trivial correlation function. If the whole system is fully coherent – i.e., one pure BEC – vortices exist in the correlation function if and only if they are there in the condensate wavefunction itself, and the study of the associated coherence vortices would be pointless. A partially coherent cloud, such as bosons in a one-dimensional or disordered potential, will also not present coherence vortices in most cases, but only a decaying correlation function. Instead, I sketch an experiment that uses the random relative phase of two independent BECs.

The experiment starts out with a pair of independent BECs, for simplicity in two dimensions. Pairs of independent BECs are created by holding atoms in two separate traps while cooling them down below the critical temperature [11]. Such pairs of BECs will produce interference patterns when brought together, but the two are statistically independent in the sense that their global phase difference – and thus the phase of the interference pat-

tern – varies randomly from shot to shot. Interference between the two independent BECs is, thus, washed out only in the average over many experimental runs. In an optical system, a beam has a finite coherence time and thus it self-averages. It is possible that one could construct something similar by making clever use of the finite coherence length of an elongated or disordered system, but I will not follow that line of thought here. I thus opt for averaging over repeated single shots as the straightforward (but tedious) way to construct an ensemble average – by hand, so to speak – in this proposed experiment.

The BECs are put in different spin states and released towards each other head on. The two spin states  $a$  will be labeled 1 and 2, respectively, and the trapping potential for each state is written as

$$V_a(\mathbf{r}) = \frac{1}{2}m\omega^2(\mathbf{r} - \mathbf{r}_{0a}), \quad (2)$$

where the trap center  $\mathbf{r}_{0a}$  is taken to be different for the two BECs. They are first Bose-Einstein condensed at a distance large enough to avoid contact, and then adiabatically brought to their starting positions,  $\mathbf{r}_{0a}$ . At time  $t = 0$  the traps are suddenly moved to target positions  $\mathbf{r}'_{0a}$ . The BECs are accelerated towards these new potential minima, and the resulting collision excites vorticity. At a final time  $t$ , the atoms of species 1 are transferred into species 2, and the resulting state is recorded. Direct observation of the density profile will reveal a set of vortices, whose positions depend on the initial, random phase difference between the two BECs. We denote this phase difference  $\Theta$ . It is in the transfer at time  $t$  that this phase difference will be decisive.

The process is simulated for a binary mixture of  $4.4 \times 10^4$  atoms of  $^{87}\text{Rb}$  equally distributed among the states  $|F, m_F\rangle = |1, 1\rangle$  and  $|F, m_F\rangle = |1, -1\rangle$ , each in a trap of frequency  $\omega = 2\pi \cdot 20 \text{ s}^{-1}$  in the plane, and in addition a tight trap of frequency  $2\pi \cdot 400 \text{ s}^{-1}$  is assumed along the  $z$  direction; this direction is integrated out so that the physics in the 2D plane is simulated. The starting positions are at  $\mathbf{r}_{01} = (12 \mu\text{m}, 0)$ , and  $\mathbf{r}_{02} = -\mathbf{r}_{01}$ , and the target positions are both at the origin,  $\mathbf{r}'_{01} = \mathbf{r}'_{02} = \mathbf{0}$ . This system is described by the two-component Gross-Pitaevskii equation,

$$\begin{aligned} i\hbar \frac{\partial}{\partial t} \Psi_1 &= \left[ -\frac{\hbar^2}{2m} \nabla^2 + V_1 + U_{11}|\Psi_1|^2 + U_{12}|\Psi_2|^2 \right] \Psi_1(\mathbf{z}) \\ i\hbar \frac{\partial}{\partial t} \Psi_2 &= \left[ -\frac{\hbar^2}{2m} \nabla^2 + V_2 + U_{22}|\Psi_2|^2 + U_{12}|\Psi_1|^2 \right] \Psi_2(\mathbf{z}) \end{aligned}$$

with  $U_{ab} = 4\pi\hbar^2 a_{ab}/m$ , where the  $s$ -wave scattering lengths are  $a_{11} = a_{22} = 100.4a_B$  and  $a_{12} = 101.3a_B$ , where  $a_B$  is the Bohr radius. A definite value of  $\Theta$  is used in each simulation run. Two examples, for different  $\Theta$ , are shown in Fig. 1. The physics of the violent collision is seen to be mainly governed by pass-through [12]

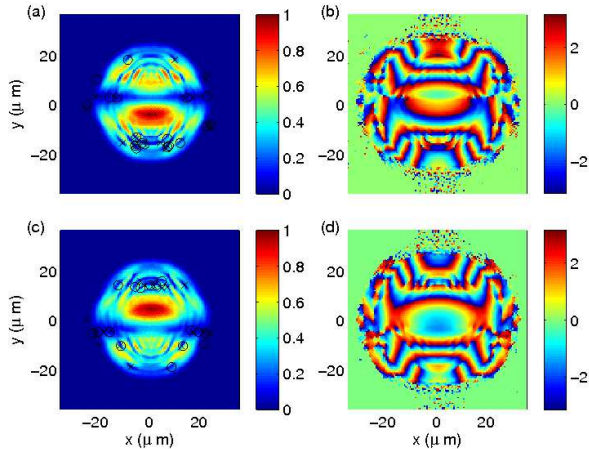


FIG. 1. [Color online] Collision of two BECs for two cases with different and randomly chosen initial phase difference. Simulation parameters as in text. Density and phase are recorded at  $t = 100$  ms. (a), (c): Density; (b), (d): Phase. (a), (b):  $\Theta = 1.98296$  radians; (c), (d):  $\Theta = 4.19545$  radians. Units for the density is such that its maximum value is 1. Positions of vortices are indicated with crosses in the figures, and antivortices with rings.

and quantum interpenetration [13]. Subsequent transfer of the population to component 1 results in a single BEC containing a set of vortex-antivortex pairs whose positions – in the Gross-Pitaevskii picture – depend on  $\Theta$ . Averaging over the phase difference will wash out the vortices. However, the vorticity in the correlation function will not. The exact correlation function after transfer is simply

$$g(\mathbf{r}, \mathbf{r}') = \Psi_1^*(\mathbf{r})\Psi_1(\mathbf{r}') + \Psi_2^*(\mathbf{r})\Psi_2(\mathbf{r}'), \quad (5)$$

since the cross-term vanishes for independent condensates. The vortices in  $g(x, y, x', y')$  corresponding to Fig. 1 are imaged in Fig. 2 as a sequence of 3D frames in the space  $(x, y, x')$ , with a fixed  $y'$  for each frame. There are vertical vortex lines visible in all four isosurfaces; these are inherited from the vorticity created in the collision (cf. [2]). In addition, a tangle is created of vortices not perpendicular to the  $xy$  plane; it is tempting to think of these as more genuine coherence vortices.

Note that before the transfer, the vorticity in the two-component system takes the form of skyrmions or filled-core vortices. However, it would be incorrect to call them coherence vortices, since their locations are independent of the phase difference  $\Theta$  and thus they are manifest directly in the density itself, even after averaging.

*Detection.* – In order to observe the coherence vortices experimentally, one must reconstruct the field-field correlation function  $g(\mathbf{r}, \mathbf{r}')$ . For cold atoms, there exists no practical method for measuring it at arbitrary coordinates. For optical systems, one may let the light pass through two pinholes and observe the phase of the re-

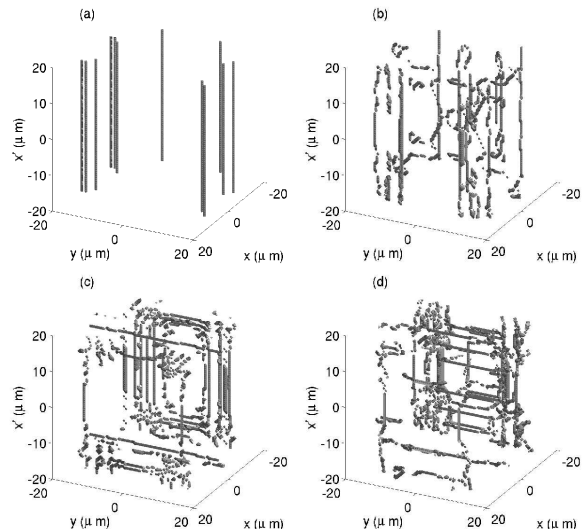


FIG. 2. Vortices (isosurfaces of the phase winding) of the correlation function  $g(x, y, x', y')$ , at three-dimensional slices of the four-dimensional space, fixed at (a)  $y' = 0$ , (b)  $y' = 3.42\mu\text{m}$ , (c)  $y' = 6.83\mu\text{m}$ , and (d)  $y' = 10.25$ , respectively. The parameters are as in Fig. 1.

sulting interference pattern. Ref. [3] mentions this type of method as an alternative also for matter systems, but does not discuss how. It is possible that a scheme could be devised where atoms in small neighborhoods of two points are excited and then brought together. Instead, one may obtain an approximate correlation function by experimentally imitating the type of averaging that is done in *c*-field calculations [14].

In a single realization, the spatial profile of the condensate's phase can be measured by letting the BEC interfere with another one initially held at a distance. (In the present scheme, this means managing three BECs, whereof two should be independent.) One can now record the set of phase differences between all points in the single run, and then average this function over repeated runs to obtain the approximate correlation function,

$$g_{\text{exp}}(\mathbf{r}, \mathbf{r}') = \langle e^{i[\theta(\mathbf{r}') - \theta(\mathbf{r})]} \rangle, \quad (6)$$

where  $\theta(\mathbf{r})$  is the phase at point  $\mathbf{r}$  inferred from the fringe pattern in a single experimental run. The approximation built into this procedure is the neglect of spatial density variations, as seen in Eq. (6). It is often a good one as far as the locations of the centermost vortices are concerned. We simulate an actual experiment by making 30 individual runs with random initial values of  $\Theta$  and random noise on the wavefunctions  $\Psi_j$  on a 5% level. In Fig. 3, the simulated correlation function  $g_{\text{exp}}$  is compared with the exact one that includes density information. The result may be improved by reading off a coarse-grained density profile from the interference fringes, if one so wishes.

The time development of the coherence vortices may now be studied by doing repeated experiments; since we

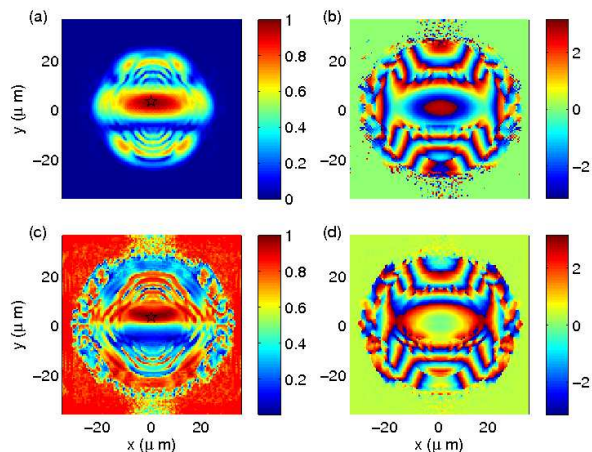


FIG. 3. [Color online] Field-field correlation function  $g(\mathbf{r}, \mathbf{r}'_0)$ , with  $\mathbf{r}_0$  fixed. The position of  $\mathbf{r}_0$  is indicated with a star. (a), (b): Exact correlation function. (c), (d): Approximate correlation function of Eq. (6), which simulates the result of the proposed experiment. (b), (d): Phase of  $g$ ; (b), (d): Absolute value  $|g|$ . Normalization is such that the maximum value of  $|g|$  is 1. The parameters are as in Fig. 1.

are studying average quantities, the destructive imaging technique is not a problem.

Correlation functions for four time instances are shown in Fig. 4. It can be seen how the behavior of the correla-

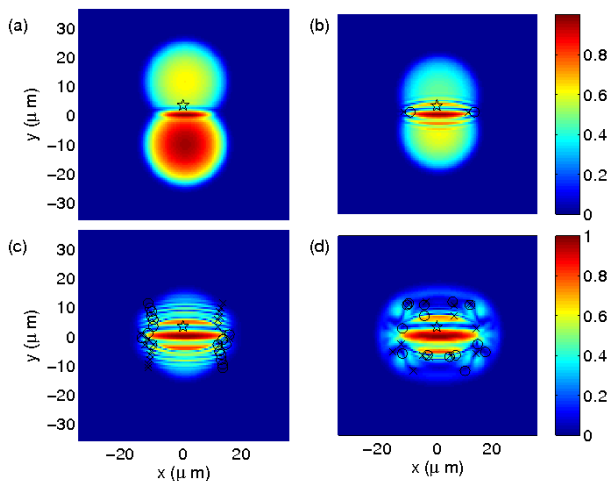


FIG. 4. [Color online] Time development of the field-field correlation function  $g(\mathbf{r}, \mathbf{r}'_0)$ , with  $\mathbf{r}_0$  fixed. The modulus  $|g(\mathbf{r}, \mathbf{r}'_0)|$  is displayed. (a): Time  $t = 25\text{ms}$ , (b):  $t = 50\text{ms}$ , (c):  $t = 75\text{ms}$ , (d):  $t = 100\text{ms}$ . Positions of coherence vortices are indicated with crosses in the figures, and antivortices with rings. The position of  $\mathbf{r}_0$  is indicated with a star. The parameters are as in Fig. 1.

tion function mirrors the physical process: two condensates approaching, colliding and interpenetrating, creating vortex-antivortex pairs in the process. This picture is made especially clear by choosing the 2D plane of view to be parallel to the physical space; as we have seen, vortex tangles move in all four dimensions.

*Concluding remarks.* – Summing up, this Letter wishes to point out two (related) reasons for studying coherence vortices in cold matter systems: It opens up for studying dynamics of vortices in high dimensions, and new types of high-dimensional topological defect, unseen in 3D, can be created here. As a specific example, a system of two colliding BECs was simulated, in which a tangle of two-dimensional coherence vortex sheets was created. A recipe for a proof-of-principle experiment was laid out where coherence vortices are created and detected using current experimental technology.

The author is indebted to Harri Mäkelä for help with homotopy groups and to Jani Martikainen for feedback on the manuscript.

- 
- [1] G. Gbur and T. Visser, *Opt. Comm.* **222**, 117 (2003).
  - [2] G. Gbur and T. Visser, *Opt. Comm.* **259**, 428 (2005).
  - [3] T. P. Simula and D. M. Paganin, *Phys. Rev. A* **84**, 052104 (2011).
  - [4] J.-P. Martikainen and H. T. C. Stoof, *Phys. Rev. A* **70**, 013604 (2004).
  - [5] G. M. Kavoulakis, S. M. Reimann, and B. Mottelson, *Phys. Rev. Lett.* **89**, 079403 (2002).
  - [6] S. M. Reimann, M. Koskinen, Y. Yu, and M. Manninen, *Phys. Rev. A* **74**, 043603 (2006).
  - [7] A. L. Fetter, *Rev. Mod. Phys.* **81**, 647 (2009).
  - [8] H. Mäkelä, Y. Zhang, and K.-A. Suominen, *J. Phys. A: Math. Gen.* **36**, 8555 (2003).
  - [9] S.-K. Yip, *Phys. Rev. A* **75**, 023625 (2007).
  - [10] T. Kibble, in *Conference of the NATO-Advanced-Study-Institute on Patterns of Symmetry Breaking*, edited by H. Arodz, J. Dziarmaga, and W. H. Zurek (Kluwer, Dordrecht, 2003), pp. 3–36.
  - [11] M. R. Andrews *et al.*, *Science* **275**, 637 (1997).
  - [12] K. Sasaki, N. Suzuki, D. Akamatsu, and H. Saito, *Phys. Rev. A* **80**, 063611 (2009).
  - [13] D. Kobayakov *et al.*, *Phys. Rev. A* **85**, 013630 (2012).
  - [14] A. Bezett, E. Toth, and P. B. Blakie, *Phys. Rev. A* **77**, 023602 (2008).